Polymer Chemistry

Accepted Manuscript

ROYAL SOCIETY OF CHEMISTRY

www.rsc.org/polymers

A new thieno-isoindigo derivative-based D–A polymer with very low bandgap for high-performance ambipolar organic thin-film transistors

Guobing Zhang,[a, c]* Zhiwei Ye,[a] Peng Li,[a, b] Jinghua Guo, [a, b] Qinghe Wang, [a, b] Longxiang Tang,[b] Hongbo Lu,[a, c] and Longzhen Qiu [a, c]*

[a]Key Lab of Special Display Technology, Ministry of Education, National Engineering Lab of Special Display Technology, State Key Lab of Advanced Display Technology, Academy of Opto-Electronic Technology, Hefei University of Technology, Hefei, 230009, China. E-mail: gbzhang@hfut.edu.cn, lzqiu@ustc.edu

[b]Department of Polymer Science and Engineering, School of Chemistry and Chemical Engineering, Hefei University of Technology, Hefei, 230009, China.

[c]Key Laboratory of Advanced Functional Materials and Devices, Anhui Province.

Abstract

A new thieno-isoindigo derivative, bis(5-oxothieno[3,2-*b*]pyrrole-6-ylidene)benzodifurandione (**BTPBF**) was synthesized by replacing the outer benzene ring of isoindigo derivative (**BIBDF**) with thiophene. This was used for the first time as an acceptor to construct a donor-acceptor polymer (**PBTPBF-BT**) for organic thin-film transistors. The thermal stability, photophysical-, and electrochemical properties, microstructure, and transistor characteristics were also investigated. Compared to isoindigo derivative-based polymer **PBIBDF-BT**, thieno-isoindigo derivative-based polymer **PBTPBF-BT** had a much smaller bandgap (0.71 eV), similar deep LUMO level, (–3.94 eV) and higher HOMO level (–5.18 eV). Therefore, when Au metal was used as the electrode and the devices were tested under similar vacuum conditions, **PBIBDF-BT** exhibited *n*-type transport, whereas **PBTPBF-BT** exhibited ambipolar transport due to the deep LUMO and suitable HOMO level. Highest mobilities of 0.45 and 0.22 $cm^2V^{-1}s^{-1}$ were obtained for hole and electron, respectively. Under the air condition, the hole mobility of **PBTPBF-BT** significantly increased to 0.61 $cm^2V^{-1}s^{-1}$ and electron mobility was maintained at 0.07 $cm^2V^{-1}s^{-1}$. Overall, this study demonstrates that by replacing the outer benzene with thiophene can effectively vary the polymer properties such as bandgap, energy levels and, as a result, tune the

transport behavior.

1. Introduction

Recently, conjugated polymers comprising alternating electron donor (D) and acceptor (A) units in the polymer backbone have attracted considerable attention all over the world because most high-performance materials for organic thin-film transistor (OTFT) applications are D–A polymers.[1] Because of the strong D–A interactions between the nearest neighboring intermolecular overlapping and ordered π–π packing of polymer chains, the introduction of a strong electron-deficient unit into D–A polymer has proven to be an effective approach to enhance the performance of OTFTs.[2] Amide-containing dyes such as isoindigo have been extensively used as acceptor units for constructing D–A polymers that exhibit high charge-carrier mobilities for both holes and electrons.[3] Recent studies have shown that the structure of isoindigo was slightly twisted because of the steric repulsion between the protons on the phenyl rings and the carbonyl oxygens of the oxindoles.[4] To avoid this steric repulsion, thieno-isoindigo was synthesized by replacing the outer phenyl rings of isoindigo with thiophenes. The short oxygen–sulfur bone distance in the thieno-isoindigo unit provides favorable interactions between the carbonyl oxygens and sulfur atoms of thiophenes, which may further enhance close intermolecular contacts and planarity along the backbone.[4c] Thieno-isoindigo-based polymers with various electron-rich units have been synthesized, and the hole mobilities are in the range 10^{-1} to 10^{-4} $cm^2V^{-1}s^{-1}$.[5] However, most thieno-isoindigo polymers have relatively high lowest unoccupied molecular orbitals (LUMO: –3.6 to –3.8 eV) and a few ambipolar/*n*-type thieno-isoindigo semiconductors have been reported.[6] A low-lying LUMO energy level (~ –4.0 eV) is required for ambipolar/*n*-type semiconductors to achieve an effective charge injection and stable electron transport.[7] In general, two methods are available for the structure modification of polymers to achieve lower LUMO energy levels. First, the addition of a strong electron-deficient group is indeed beneficial to achieve lower LUMO energy levels.[8] For example, the fluorination of isoindigo can reduce the LUMO energy levels of the polymers and affords high-performance ambipolar polymers.[9] Second, an electron-deficient side

chain can also lower the LUMO energy levels of the polymers, and the corresponding OTFTs exhibit ambipolar or *n*-type charge transport.[10]

Besides the above mentioned points, the incorporation of an electron-deficient moiety into the π-conjugated backbone not only affects the LUMO energy levels but also extends the conjugation and enhances the intramolecular and intermolecular interactions of the polymers.[11] Bis(2-oxoindolin-3-ylidene)benzodifurandione (**BIBDF**) is an excellent isoindigo derivative because a strong electron-deficient benzodifurandione moiety is incorporated. The polymers based on **BIBDF** exhibited deep LUMO energy levels, low bandgaps and remarkable ambipolar/n-type charge transport.[12] We have previously demonstrated that BIBDF-based D–A polymers are promising as semiconductor layer for applications in OTFTs.[12a,f] We currently synthesized another isoindigo derivative (**BTPBF**) by replacing the outer benzene rings of **BIBDF** with thiophenes (Fig. 1), an obvious next step, and began studies using as the acceptor unit in D–A polymer semiconductors. The geometry of **BTPBF** should decrease the steric repulsion between neighboring backbone units, and potentially attractive sulfur−oxygen interactions may assist in backbone planarization.[5a,13] Therefore, **BTPBF**-based D–A polymers should exhibit smaller bandgaps than the corresponding **BIBDF**-based polymers and potentially also have close π-π stacking.

In this paper, we report the synthesis of thieno-isoindigo derivative **BTPBF** and its D–A polymer (**PBTPBF-BT**), and characterize of the thermal, optical, electrochemical, microstructure, and OTFTs properties of the polymer for the first time. The reported polymer **PBIBDF-BT** (Scheme 1), in which the outer ring is benzene was used for comparison. Consequently, compared to **PBIBDF-BT**, **PBTPBF-BT** exhibited a much smaller bandgap (0.71 vs 1.18 eV), a similar deep LUMO energy level (–3.94 vs –4.03 eV), and a higher HOMO energy level (–5.18 vs –5.55 eV). As a result, when Au metal was used as the electrode, and the devices were tested under the same vacuum conditions, **PBIBDF-BT** exhibited *n*-type transport, whereas **PBTPBF-BT** exhibited ambipolar transport due to a suitable HOMO level. The hole and electron mobilities were as high as 0.45 and 0.22 $cm^{-1}V^{-1}s^{-1}$,

respectively. While evaluated under air, **PBTPBF-BT** still exhibited ambipolar behavior, and maintained the electron mobility of up to 0.07 $cm^2V^{-1}s^{-1}$, along with significantly increased hole mobility of over 0.61 $cm^2V^{-1}s^{-1}$. This study demonstrated that by replacing the outer benzene with thiophene, the polymer properties such as bandgap, energy levels can be varied and, as a result the transport behavior can be tuned.

2. Results and discussion

2.1. Synthesis and characterization

The synthetic routes for the monomers are shhown in Scheme 1. Starting from 3-bromothiophene, compound **1** was conveniently synthesized by Ullmann coupling reaction. Then, Friedel–Crafts reaction with oxalyl chloride afforded the diketopyrrole precursor **2**. The resulting diketone compound was reacted with benzodifurandione to afford thieno-isoindigo derivative **3** (**BTPBF**) in a low yield. The **BTPBF** monomer was easily converted to dibromo-monomer **4** with *N*-bromosuccinimide (NBS) in a tetrahydrofuran (THF) solution at room temperature. Finally, **PBTPBF-BT** was synthesized by Stille cross-coupling reaction in the presence of $Pd_2(dba)_3$ as the catalyst and P(*o*-tolyl)$_3$ as the ligand (Scheme 1). Although alkyl chains on donor and large branched chains on acceptor were introduced for solubility, **PBTPBF-BT** has limited solubility in THF, chloroform, chlorobenzene, and dichlorobenzene, indicating the very strong intermolecular interactions due to the large fused **BTPBF** units. The number-average molecular weight (Mn) and PDI of the polymer was determined by gel permeation chromatography (GPC) using polystyrenes as the standard and trichlorobenzene as the eluent. The Mn was 22.4 kDa with a polydispersity of 1.81 for **PBTPBF-BT**. The TGA curve is shown in Fig. 2. The decomposition temperature (Td) at 5% weight loss for polymers was above 370 ^oC, sufficient for device fabrication. DSC curve clearly showed endothermic peaks at -22.6 ℃ during heating up, and corresponding exothermic peaks at -26.8 and 77.0 ℃ were also observed when they were cooled down. The transition temperatures of the polymer should be attributed to the phase transition temperature caused by the melting of the alkyl chains. This might be the strong intermolecular interactions which result in clear main-chain and

side-chain phase separation. The high transition temperature was the melting of long branched chain, and the low one was the melting of dodecyl chain.

2.2. Optical and electrochemical properties

The normalized UV−vis−NIR absorption spectra of the polymers in dilute chlorobenzene solution and as thin films casted from solution are shown in Fig. 3. The corresponding results are shown in Table 1. **PBTPBF-BT** showed a typical dual-band consisting of a sharp band at high-energy region and a more intense, broader band at low-energy region. In solution, **PBTPBF-BT** exhibited a maximum absorption peak ($\lambda_{\max}^{abs}$) at ~1107 nm and an absorption band-edge (λ_{onset}^{abs}) at ~1640 nm, respectively. As a comparison, although the maximum absorption of the film showed no red-shift, the absorption of the film was more broad and a slight shoulder peak was located at ~1300 nm both indicating that the solid film should be well arranged and aggregated owing to the strong intramolecular and intermolecular interactions, which may facilitate charge transport. The absorption spectra of **PBTPBF-BT** both in solution and film were more red-shifted than those of isoindigo derivative-based polymer **PBIBDF-BT**. The optical bandgap (E_g^{opt}) of **PBTPBF-BT** film calculated from the absorption edge (~1750 nm) was 0.71 eV. As predicted, the bandgap of **PBTPBF-BT** was also much smaller than that of the analogous isoindigo derivative-based polymer **PBIBDF-BT** (1.18 eV) with the same donor unit.[12a] The low bandgap for **PBTPBF-BT** is among the lowest reported for D−A polymers to date, and is in the class of the reported bandgaps.[5a, 14]

The electrochemical properties of **PBTPBF-BT** was characterized by cyclic voltammetry (CV). The cyclic voltammogram is shown in Fig. 4a. The potentials were referenced to Ag/Ag^+ and the redox Fc/Fc^+ was assumed as an absolute energy level of 4.8 eV to vacuum. The redox Fc/Fc^+ was measured under the same conditions as the polymer film and located at 0.05 V related to Ag/Ag^+ electrode. **PBTPBF-BT** clearly exhibited both *p*- and *n*-doping processes, in which the oxidative peaks were stronger than those of the reductive peaks. The onset oxidation potential (E_{onset}^{ox}) and

onset reduction potential (E_{onset}^{red}) of **PBTPBF-BT** were located at 0.43 and -0.81 V, respectively. The HOMO and LUMO energy levels were calculated to be –5.18 and –3.94 eV for **PBTPBF-BT**, respectively. The energy level diagrams are shown in Fig. 4b, compared to the energy level of **PBIBDF-BT**, **PBTPBF-BT** had a similar deep LUMO energy level. This can be attributed to electron-deficient benzodifurandione moiety in the polymer backbone which greatly lowered the LUMO energy level. The HOMO energy level was much higher ~0.37 eV, after replacing the outer benzene ring with thiophene. For OTFT applications, a deep LUMO energy level is beneficial to facilitate charge injection and stable electron transport, and a suitable HOMO energy level is beneficial to hole injection. Hence, ambipolar charge transport is expected in **PBTPBF-BT**-based OTFT devices when an appropriate single metal with a Fermi energy level between 4.0 eV and 5.2 eV (e.g., Au) is used. Compared to the corresponding benzene-isoindigo derivative analog **PBIBDF-BT** (HOMO: –5.55 eV),[12a] the thiophene-isoindigo derivative **PBTPBF-BT** has potentially a low hole injection barrier because of a suitable HOMO energy level. The differences between the electrochemical and optical properties of thiophene-isoindigo derivative and isoindigo derivative-based polymers are induced by the stronger electron-donating properties of the thiophene ring compared to the benzene ring. Moreover, coplanarity with the neighboring aromatic units is easier, whilst steric hindrance is also reduced.[5a]

2.3. Microstructure

To provide further insight into the microstructure of the polymer, X-ray diffraction (XRD) was used to investigate the structural ordering of the films. The XRD patterns showed the out of plane reflections attributed to lamellar type crysrallinity for polymer film drop-casted on silicon substrates (Fig. 5). the crystallographic parameters are listed in Table S1. **PBTPBF-BT** exhibited a strong diffraction peak (100) and also well defined (200), (300) and (400) diffraction peaks in the XRD pattern. The presence of ordered reflection indicates that the polymer has a layer-by-layer lamellar structure. The (100) diffraction peak at $2\theta = \sim 3.36^{o}$ indicates that the corresponding lamellar spacing was 26.3 Å. Besides the (100)–(300)

reflection peaks, the film also exhibited a (010) diffraction peak at 2θ = ~ 25.28°, which was attributed to the π–π stacking. The calculated π–π stacking distance of **PBTPBF-BT** was 3.52 Å. The small π-π stacking indicates the stronger intramolecular D-A interactions between the fused **BTPBF** and the dithiophene unit and the strong intermolecular interaction of polymer backbone. Upon thermal annealing at 150 and 180 °C, the diffraction peaks ((100)–(200)) of annealed film became noticeably sharper. This indicates that the annealed films of **PBTPBF-BT** had more crystalline domains and better lamellar structures than those of the as-cast film, which are the desired properties for achieving a higher mobility in OTFTs devices.

2.4. OTFTs performance

To test the field-effect performance, bottom-gate/top-contact transistors were fabricated with thieno-isoindigo derivative-based polymer as the semiconductor layer on the fluoropolymer Cytop-treated SiO_2/Si substrate. The polymer films were subsequently annealed at different temperatures (150 and 180 °C) in glove box under nitrogen atmosphere. The preliminary device performances of polymers are listed in Table S2. The evaluation of OTFTs were carried out under vacuum (3×10^{-4} mbar). **PBIBDF-BT** exhibited *n*-channel transport under this vacuum condition (Figure S2). This is probably because of the large hole injection barrier between their low-lying HOMO levels and the work function of Au under this vacuum conditions. When the devices tested under air or low vacuum, the large hole injection barrier can be reduced by the oxygen doping, therefore, **PBIBDF-BT** exhibited ambipolar transport under air or low vacuum. The results are consistent with other reports in that the OTFT devices with PMMA encapsulation (isolated from the air) exhibited typical *n*-channel characteristics, otherwise showed ambipolar transport.[12b] In contrast, the deep LUMO energy level and suitable HOMO energy level of **PBTPBF-BT** should provide effective injection for both electron and hole; therefore, ambipolar transport was observed in **PBTPBF-BT**-based OTFTs, as shown in Fig. 6. The V-shape transfer curves are shown in hole-enhancement and electron-enhancement mode operations in Figs. 6c and d, respectively. The mobilities were calculated from the respective saturation regime of transfer curves, and the corresponding device performances are

listed in Table S2. The nonannealed (N/A) devices exhibited the highest hole mobility of 0.13 $cm^2V^{-1}s^{-1}$ and electron mobility of 0.08 $cm^2V^{-1}s^{-1}$, respectively. For **PBTPBF-BT**, the thermal annealing was an effective way to optimize the device performances. After 150 ^oC annealing, the highest hole and electron mobilities increased to 0.34 and 0.13 $cm^2V^{-1}s^{-1}$, respectively. With further increase in the annealing temperature to 180 ^oC, the highest hole mobility increased to 0.45 $cm^2V^{-1}s^{-1}$ and the electron mobility slightly increased to 0.22 $cm^2V^{-1}s^{-1}$.

The devices were also evaluated under air, and the corresponding data are listed in Table S3. As shown in Fig. 7, **PBTPBF-BT** still exhibited ambipolar transport characteristics. Because of the oxygen doping of the polymer film, the hole mobilities of **PBTPBF-BT** significantly increased. The highest hole mobility of 0.61 $cm^2V^{-1}s^{-1}$ and an average mobility of 0.53 $cm^2V^{-1}s^{-1}$ were obtained while the highest electron mobility decreased to 0.07 $cm^2V^{-1}s^{-1}$.

Compared to **PBIBDF-BT**, **PBTPBF-BT** had a similar deep LUMO energy level, but more suitable HOMO energy level for achieving ambipolar characteristics. The strong D-A intramolecular and intermolecular interactions, the long-range-ordered structure and close π–π stacking should all contribute to the excellent ambipolar transport. However, the mobilities of the thiophene-isoindigo derivative-based **PBTPBF-BT** was lower than those of the reported isoindigo derivative-based polymers.[12] This is mainly because of the relatively low molecular weight of **PBTPBF-BT** which significantly affected the OTFT performances. The polymer semiconductor with a high molecular weight usually exhibited a high field-effect performance than those of the lower ones.[15]

The mobility with/without annealing depended on the morphology of the polymer thin film, as shown in Fig. 8. The topographic and phase images of the **PBTPBF-BT** thin-films show that the N/A polymer thin film comprised of fine, clustered and nanofiber crystals in whole areas. when annealed at 180 ^oC, the polymer film exhibited large and continuous nanofibrillar structures and formed an interconnected polymer network that formed an efficient pathway for charge-carrier transport, resulting in enhanced charge-carrier mobilities.

3. Conclusion

A new thieno-isoindigo derivative (BTPBF) and its polymer (PBTPBF-DT) were designed and synthesized for the first time by replacing the outer benzene ring with the thiophene of isoindigo derivative. The results indicate that the replacement of the outer benzene ring with thiophene significantly affected the absorption spectrum, bandgap, and HOMO level. Consequently, **PBTPBF-BT** exhibited ambipolar characteristics because of the deep LUMO level and suitable HOMO level. The devices exhibited a hole mobility of as high as 0.45 $cm^2V^{-1}s^{-1}$ and an electron mobility of over 0.22 $cm^2V^{-1}s^{-1}$ under vacuum conditions. Under the air condition, the hole mobility of **PBTPBF-BT** significantly increased to 0.61 $cm^2V^{-1}s^{-1}$ and electron mobility was maintained at 0.07 $cm^2V^{-1}s^{-1}$. This study demonstrated that (i) the replacement of the outer benzene with thiophene can effectively tune the polymer properties such as bandgap, energy level and, as a result, vary the transport behavior; (ii) The BTPBF unit with strong electron-deficient nature may be an useful new dye for the construction of low-bandgap conjugated polymers and applications in high-performance OTFTs and other optoelectronic devices; (iii) PBTPBF-BT with a low-lying LUMO energy level for electron injection and transport, suitable HOMO energy level for hole injection, long-range ordered lamellar crystalline structure and close π–π stacking may be an useful ambipolar semiconductor for OTFTs.

4. Experimental

4. 1. Instrumentation

Nuclear magnetic resonance (NMR) spectra were recorded on a Mercury plus 600 MHz machine. Thermo-gravimetric analyses (TGA) were conducted with a TA Instruments QS000IR at a heating rate of 10 $^oC\ min^{-1}$ under nitrogen gas flow. Differential scanning calorimetry (DSC) was conducted under nitrogen using a TA instrument Q2000. The sample (about 5 mg in weight) was first cool down to -65 ^oC, then heated up to 250 ^oC and held for 2 min to remove thermal history, followed by the cooling rate of 10 ^oC /min to -65 ^oC and then heating rate of 10 ^oC/min to 250 ^oC in all cases. Molecular weight and polydispersity index (PDI) were determined by gel permeation chromatography (GPC) analyses on a Waters Series 1525 gel at 100 ^oC

using 1,2,4-trichlorobenzene as eluent with polystyrene as standard. Absorption spectra were taken on a Perkin-Elmer model λ 20 UV-vis-NIR spectrophotometer. Electrochemical measurements were conducted on a CHI 660D electrochemical analyzer under nitrogen in a deoxygenated anhydrous acetonitrile solution of tetra-*n*-butylammonium hexafluorophosphate (0.1 M). A platinum electrode was used as a working electrode, a platinum-wire was used as an auxiliary electrode, and an Ag/Ag^+ electrode was used as a reference electrode. Polymer film was coated on the surface of platinum electrode and the ferrocene was chosen as a reference. The X-ray diffraction (XRD) data were collected from a TTRAX3 focus diffractometer with Cu Kα beam (40 KV, 200 mA) at a scanning rate of $2^o\,min^{-1}$. The solution was drop cast onto SiO_2/Si substrates. The films were then dried on a hot plate in glovebox. The atomic force microscope (AFM) measurements were performed on a SPA300HV instrument with a SPI3800 controller (Seiko Instruments).

4.2. Fabrication and characterization of field-effect transistors

Top-contact and bottom-gate OTFTs devices were fabricated in this work. A 40-45 nm-thick fluoropolymer Cytop was spin-coated onto SiO_2/Si substrate, hence Cytop/SiO_2 and Si work as gate-dielectric and gate-electrode, respectively. A chloroform solution containing semiconductor polymer was dropped onto the Cytop thin film and spin-coated. The polymer films were subsequently annealed (150 and 180 ^oC) in nitrogen. Au source-drain electrodes were prepared by thermal evaporation. The OTFT device had a channel length (L) of 100 μm and channel width (W) of 800 μm. The evaluations of the OTFTs were used a Keithley 4200 parameter on probe stage and performed in vacuum and air conditions, respectively. The electron (μ_e) and hole (μ_h) mobilities were obtained by the following equation for the saturation regime: $I_d = (W/2L)C_i\mu_{h\text{ or }e}(V_g\text{-}V_{th})^2$, where W/L is the channel width/length, I_d is the drain current in the saturated regime, C_i is the capacitance (1×10^{-8} F/cm^2) of Cytop/SiO_2 gate-dielectric, and V_{th} is the threshold voltage.

4.3. Materials

3-Bromothiophene was obtained from Darui Chemical Co. Ltd., Shanghai, China. Other chemicals used in this work were purchased from Sigma-Aldrich Chemical

Company, Alfa Aeasar Chemical Company and Sinopharm Chemical Reagent Co. Ltd., China. Chemical regents were purchased and used as received. Tetrahydrofuran (THF) and toluene were freshly distilled over sodium wire under nitrogen prior to use. 5,5′-Bis(trimethylstannyl)-3,3′-bis(dodecyl)-2,2′-bithiophene, compound **1** and **2** were synthesized via published procedures.[5,16]

4.4. Synthesis of monomers and polymer

4.4.1 Synthesis of compound 3

Compound **2** (3.39 g, 6.93 mmol), benzo[1,2-*b*:4,5-*b*']difuran-2,6(3*H*,7*H*)-dione (0.66 g, 3.47 mmol), TsOH H_2O (0.19 g， 0.97 mmol) were dissolved in acetic acid (15 mL). The mixture was refluxed for 24 h under nitrogen. After cooled to room temperature, the reaction mixture was filtered and washed with methanol. The residue was purified by flash chromatography on silica gel (hexanes: dichloromethane = 1:1). The product was obtained as a dark solid (0.42 g, 10.7%). ^{1}HNMR (600 MHz, $CDCl_3$, ppm) δ = 8.98 (s, 2H), 7.70 (d, 2H), 6.75 (d, 2H), 3.65 (d, 4H), 1.85 (s, 2H), 1.02-1.50 (m, 80H), 0.80-0.95 (t, 12H). ^{13}C (150 MHz, $CDCl_3$): δ = 172.6, 171.9, 158.1, 153.8, 142.4, 134.5, 127.8, 119.4, 118.1, 113.9,111.9, 48.9, 39.8, 34.6, 34.5, 34.2, 32.6, 32.33, 32.31, 32.29, 32.27, 32.25, 32.20, 31.99, 31.97, 29.10, 25.32, 16.73. Elemental Analysis: calcd for $C_{70}H_{104}N_2O_6S_2$ (%): C, 74.16, H, 9.25, N, 2.47, found (%): C, 73.98, H, 9.13, N, 2.21. m/z =1133.

4.4.2 Synthesis of compound 4.

N-bromosuccinimide (NBS) was added to a solution of compound **3** (0.42 g, 0.37 mmol) in THF (20 mL) under nitrogen at room temperature. The reaction was monitored by thin-film chromatography (TLC). After completion, the mixture was poured into water and extracted with dichloromethane (3×50 mL). The organic layer was washed and dried over anhydrous $MgSO_4$. Solvent was removed under reduced pressure and the residue was purified by flash chromatography on silica gel (hexanes: dichloromethane= 3: 1). The product was obtained as a dark solid (0.40 g, 83.9%). ^{1}HNMR (600 MHz, $CDCl_3$, ppm) δ = 8.65 (s, 2H), 6.60 (d, 2H), 3.65 (d, 4H), 1.78 (m, 2H), 1.20-1.40 (m, 80H), 0.88 (t, 12H). ^{13}C (150 MHz,$CDCl_3$) : δ = 171.9, 171.2, 156.9, 153.4, 132.6, 132.2, 127.5, 118.3, 118.1, 117.5, 111.6, 48.9, 39.9, 34.6, 34.1,

32.7, 32.4, 32.35, 32.3, 32.0, 29.1, 25.4, 16.8. Elemental Analysis: calcd for $C_{70}H_{102}Br_2N_2O_6S_2$ (%): C, 65.10, H, 7.96, N, 2.17, found (%): C, 64.98, H, 7.87, N, 2.01. m/z 1290 ($[M+H]^+$).

4.4.3 Synthesis of polymer PBTPBF-BT.

$Pd_2(dba)_3$ (0.0034 g, 0.0037 mmol), P(*o*-tolyl)$_3$, (0.0045 g, 0.0146 mmol) were added to a solution of 5,5′-bis(trimethylstannyl)-3,3′-bis(dodecyl)-2,2′-bithiophene (0.101 g, 0.122 mmol) and compound **4** (0.158 g, 0.122 mmol) in toluene (6 mL) under nitrogen. The solution was subjected to three cycles of admission and evacuation of nitrogen. The mixture was then heated to 110 ^oC for 48 h. After cooled to room temperature, the mixture was poured into methanol and stirred for 2 h. A black precipitate was collected by filtration. The product was purified by washing with methanol and dichloromethane in a Soxhlet extractor for 24 h each. It was extracted with hot chloroform in an extractor for 24 h. After removing solvent, a black solid was collected (0.15 g, 75.3%). Elemental Analysis: calcd for $(C_{102}H_{156}N_2O_6S_4)_n$ (%): C, 75.01, H, 9.55, N, 1.72, found (%): C, 74.55, H, 9.48, N, 1.68. Mn = 10.98 kDa, PDI = 1.86.

Acknowledgements

This work was supported by National Nature Science Foundation of China (NSFC Grant Nos. 21204017, 51203039, 21174036), Major State Basic Research Development Program of China (2012CB723406), the Program for New Century Excellent Talents in University (NCET-12-0839) and the Fundamental Research Funds for the Central Universities.

References

1 (a) H. Chen, Y. Guo, G. Yu, Y. Zhao, J. Zhang, D. Gao, H. Liu and Y. Liu, *Adv. Mater.*, 2012, **24**, 4618; (b) J. Li, Y. Zhao, H. Tan, Y. Guo, C.-A. Di, G. Yu, Y. Liu, M. Lin, S. Lim, Y. Zhou, H. Su and B.Ong, *Sci. Rep.*, 2012, **2**, 754; (c) I. Kang, H. Yun, D. Chung, S. Kwon and Y. Kim, *J. Am. Chem. Soc.*, 2013, **135**, 14896; (d) X. Zhan, Z.

Tan, B. Domercq, Z. An, X. Zhang, S. Barlow, Y. Li, D. Zhu, B. Kippelen and S. R. Marder, *J. Am. Chem. Soc.*, 2007, **129**, 7246.

2 (a) J. Park, E. Jung, J. Jung and W. Jo, *Adv. Mater.*, 2013, **25**, 2583; (b) M. Chen, O. Lee, J. Niskala, A. Yiu, C. Tassone, K.Schmidt, P. Beaujuge, S. Onishi, M. Toney, A. Zettl and J. M. Frechet, *J. Am. Chem. Soc.*, 2013, **135**, 19229; (c) X. Zhao, L. Ma, L. Zhang, Y. Wen, J. Chen, Z. Shuai, Y. Liu and X. Zhan, *Macromolecules*, 2013, **46**, 2152.

3 (a) J. Mei, Do H. Kim, A. Ayzner, M. Toney and Z. Bao, *J. Am. Chem. Soc.*, 2011, **133**, 20130; (b) T. Lei, J. Dou, J. Pei, *Adv. Mater.*, 2012, **24**, 6457; (c) R. Stalder, J. Mei, K. R. Graham, L. A. Estrada and J. R. Reynolds, *Chem. Mater.*, 2014, **26**, 664; (d) E. Wang, W. Mammo and M. R. Andersson, *Adv. Mater.*, 2014, **26**, 1801.

4 (a) G. Dutta, A. Han, J. Lee, Y. Kim, J. H.Oh and C. Yang, *Adv. Funct. Mater.*, 2013, **23**, 5317; (b) S. Li., Z. Yuan, J. Yuan, P. Deng, Q. Zhang and B. Sun, *J. Mater. Chem. A.*, 2014, **2**, 5427.

5 (a) G. Van. Pruissen, F. Gholamrezaie, M. M. Wienk and R. A. J. Janssen, *J. Mater. Chem.*, 2012, **22**, 20387; (b) M. S. Chen, J. R. Niskala, D. A. Unruh, C. K. Chu, O. P. Lee and J. M. J. Fréchet, *Chem. Mater.*, 2013, **25**, 4088; (c) Y. Koizumi, M. Ide, A. Saeki, C. Vijayakumar, B. Balan, M. Kawamoto and S. Seki, *Polym. Chem*., 2013, **4**, 484.

6 R. S. Ashraf, A. J. Kronemeijer, D. I. James, H. Sirringhaus and I. McCulloch, *Chem. Commun.*, 2012, **48**, 3939.

7 (a) J. Zaumseil, H. Sirringhaus, *Chem. Rev.*, 2007, **107**, 1296; (b) J. E. Anthony, A. Facchetti, M. Heeney, S. R. Marder and X. Zhan, *Adv. Mater.*, 2010, **22**, 3876; (c) X. Zhan, A. Facchetti, S. Baelow, T. J. Marks, M. A. Ratner, M. R. Wasielewski and S. R. Marder, *Adv. Mater.*, 2011, **23**, 268; (d) X. Zhao and X. Zhan, *Chem. Soc. Rev.*, 2011, **40**, 3278.

8 (a) Y. Wen and Y. Liu, *Adv. Mater.*, 2010, **22**, 1331; (b) F. Grenier, P. Berrouard, J.-R. Pouliot, H.-R. Tseng, A. J. Heeger and M. Leclerc, *Polym. Chem.*, 2013, **4**, 1836.

9 T. Lei, J. H. Dou, Z. J. Ma, C. H. Yao, C. J. Liu, J. Y. Wang and J. Pei, *J. Am. Chem Soc*., 2012, **134**, 20025.

10 (a) S. Li, L. Ma, C. Hu, P. Deng, Y. Wu, X. Zhan, Y. Liu and Q. Zhang, *Dyes. Pigm.*, 2014, **109**, 200; (b) P. Deng, L. Liu, S. Ren, H. Li and Q. Zhang, *Chem. Commun.*, 2012, **48**, 6960.

11 (a) J.-H. Kim, H. U. Kim, I.-N. Kang, S. K. Lee, S.-J. Moon, W. S. Shin and D.-H. Hwang, *Macromolecules*, 2012, **45**, 8628; (b) T. Lei, J. H. Dou, X. Y. Cao, J. Y. Wang and J. Pei, *J. Am. Chem. Soc.*, 2013, **135**, 12168.

12 (a) G. Zhang, P. Li, L. Tang, J. Ma, X. Wang, H. Lu, B. Kang, K. Cho, L. Qiu, *Chem. Commun.*, 2014, **50**, 3180; (b) Z. Yan, B. Sun, Y. Li, *Chem. Commun.*, 2013, **49**, 3790; (c) T. Lei, J. H. Dou, X. Y. Cao, J. Y. Wang and J. Pei, *Adv. Mater.*, 2013, **25**, 6589; (d) J.-H. Dou, Y.-Q. Zheng, T. Lei, S.-D. Zhang, Z. Wang, W.-B. Zhang, J.-Y. Wang and J. Pei, *Adv. Fucnt. Mater.*, 2014, **24**, 6270; (e) T. Lei, J.-Y. Wang and J. Pei, *Acc. Chem. Res.*, 2014, **47**, 1117; (f) G. Zhang, J. Guo, M. Zhu, P. Li, H. Lu, K. Cho and L. Qiu, *Polym. Chem*., 2015, 6, 2531.

13 X. Guo, N. Zhou, S. J.Lou, J. W. Hennek, O. Ponce, M. R. Butler, P. L. Boudreault, J. Strzalka, P. O. Morin, M. Leclerc, J. T. Lopez Navarrete, M. A. Ratner, L. X. Chen, R. Chang, A. Facchetti and T. J. Marks, *J. Am. Chem. Soc*., 2012, **134**, 18427.

14 (a) T. T. Steckler, P. Henriksson, S. Mollinger, A. Lundin, A.Salleo and M. R. Andersson, *J. Am. Chem. Soc*., 2014, **136**, 1190; (b) E. Zhou, Q. Wei, S. Yamakawa, Y. Zhang, K. Tajima, C. Yang and K. Hashimoto, *Macromolecules*, 2010, **43**, 821.

15 H.-R. Tseng, L. Ying, B. B. Y. Hsu, L. A. Perez, C. J. Takacs, G. C. Bazan and A. J. Heeger, *Nano. Lett.*, 2012, **12**, 6353.

16 X. Guo, M. D. Watson, *Org. Lett.*,2008, **10**, 5333.

Figure captions

Scheme 1 Synthetic route to the monomers and polymers.

Fig. 1 Molecular structures of isoindigo (left) and thieno-isoindigo (right) derivatives.

Fig. 2 TGA curve of polymer with a heating rate of 10 ^{o}C/min.

Fig. 3 UV-vis-NIR absorption spectra of polymers in solutions and as thin films.

Fig. 4 Cyclic voltammogram of polymer thin-film and energy level diagrams.

Fig. 5 X-ray diffraction patterns of drop-cast films of polymer.

Fig. 6 Output (a, b) and (c, d) transfer characteristics of **PBTPBF-BT** annealed at 180 ^{o}C and tested under vacuum conditions.

Fig. 7 Output (a, b) and (c, d) transfer characteristics of **PBTPBF-BT** annealed at 180 ^{o}C and tested under air conditions.

Fig. 8 AFM images (2 μm × 2 μm) of **PBTPBF-BT** thin film on Cytop-modified Si/SiO_2 substrates with and without annealing: height images (a and b), phase images (c and d).

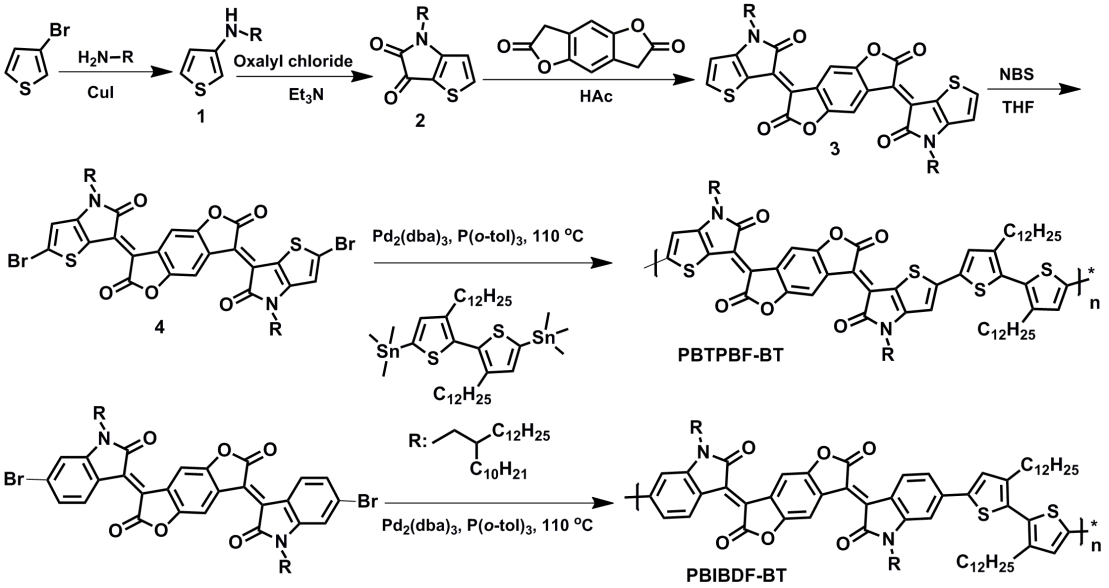

Scheme 1 Synthetic route to the monomers and polymers.

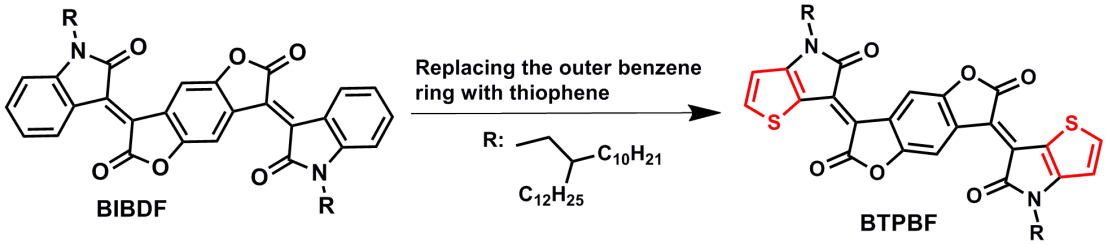

Fig. 1 Molecular structures of isoindigo (left) and thieno-isoindigo (right) derivatives.

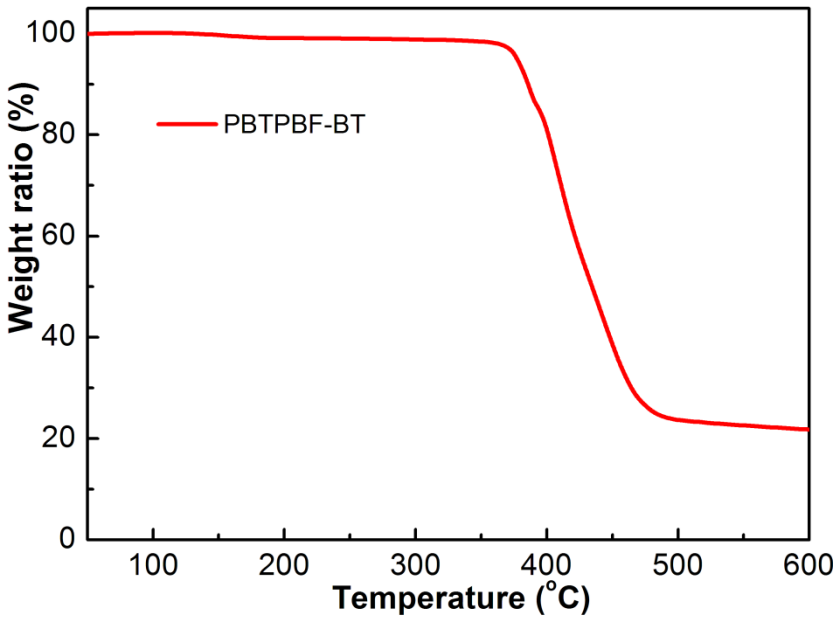

Fig. 2 TGA curve of polymer with a heating rate of 10 °C/min.

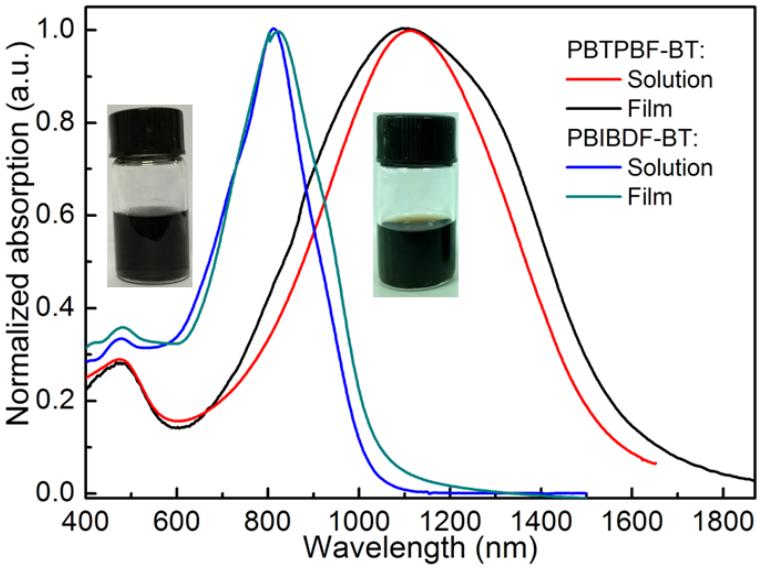

Fig. 3 UV-vis-NIR absorption spectra of polymers in solutions and as thin films.

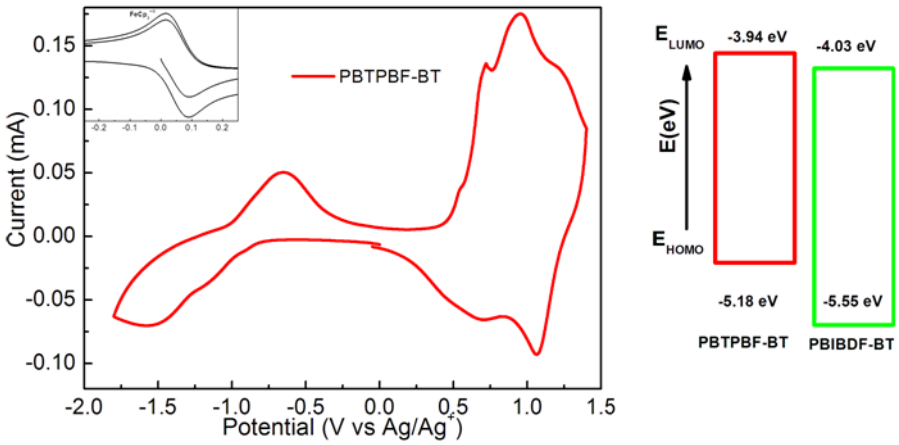

Fig. 4 Cyclic voltammogram of polymer thin-film and energy level diagrams.

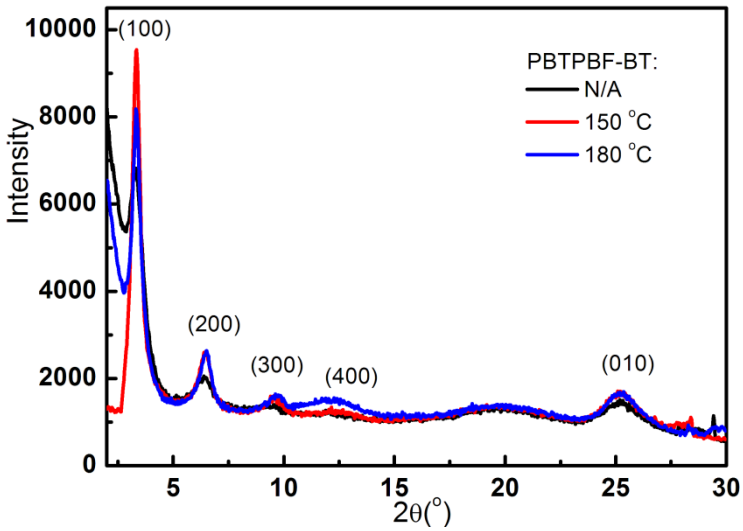

Fig. 5 X-ray diffraction patterns of drop-cast films of polymer.

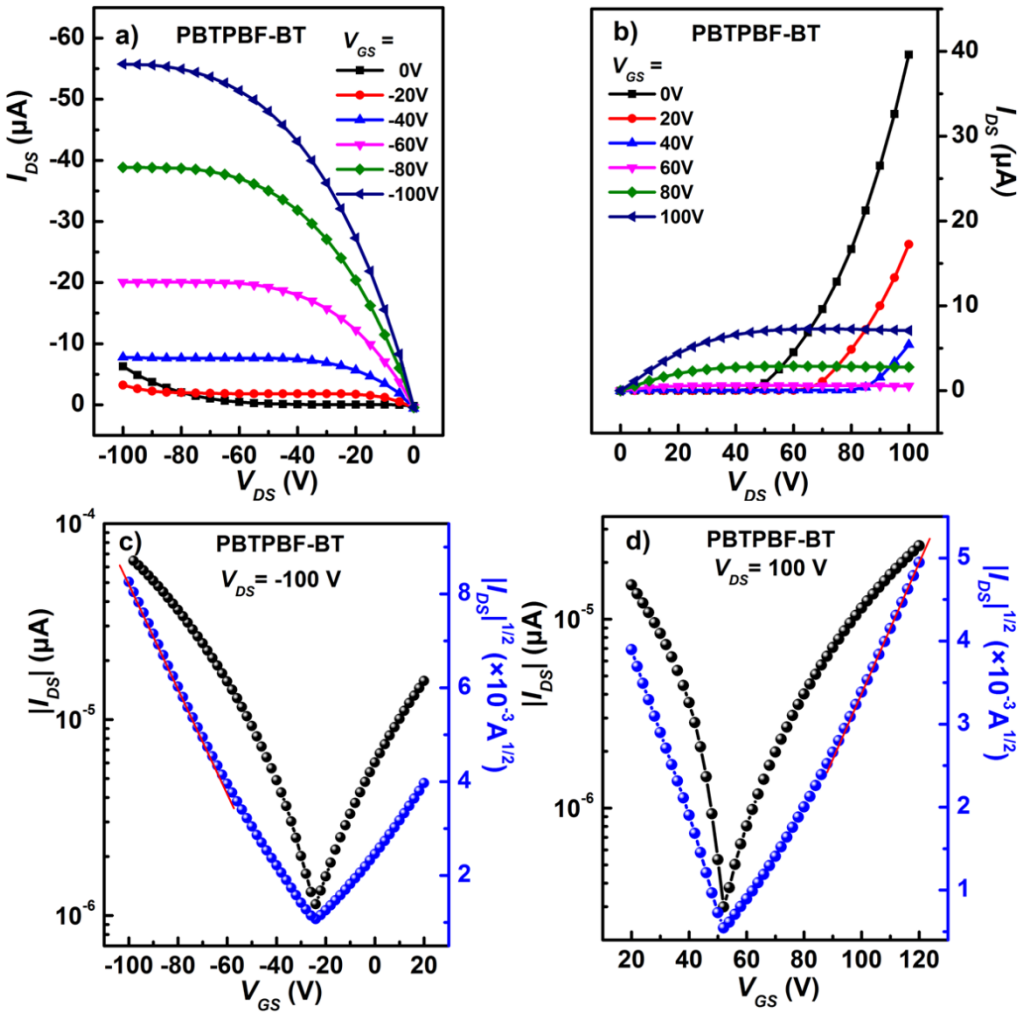

Fig. 6 Output (a, b) and (c, d) transfer characteristics of **PBTPBF-BT** annealed at 180 ^{o}C and tested under vacuum conditions.

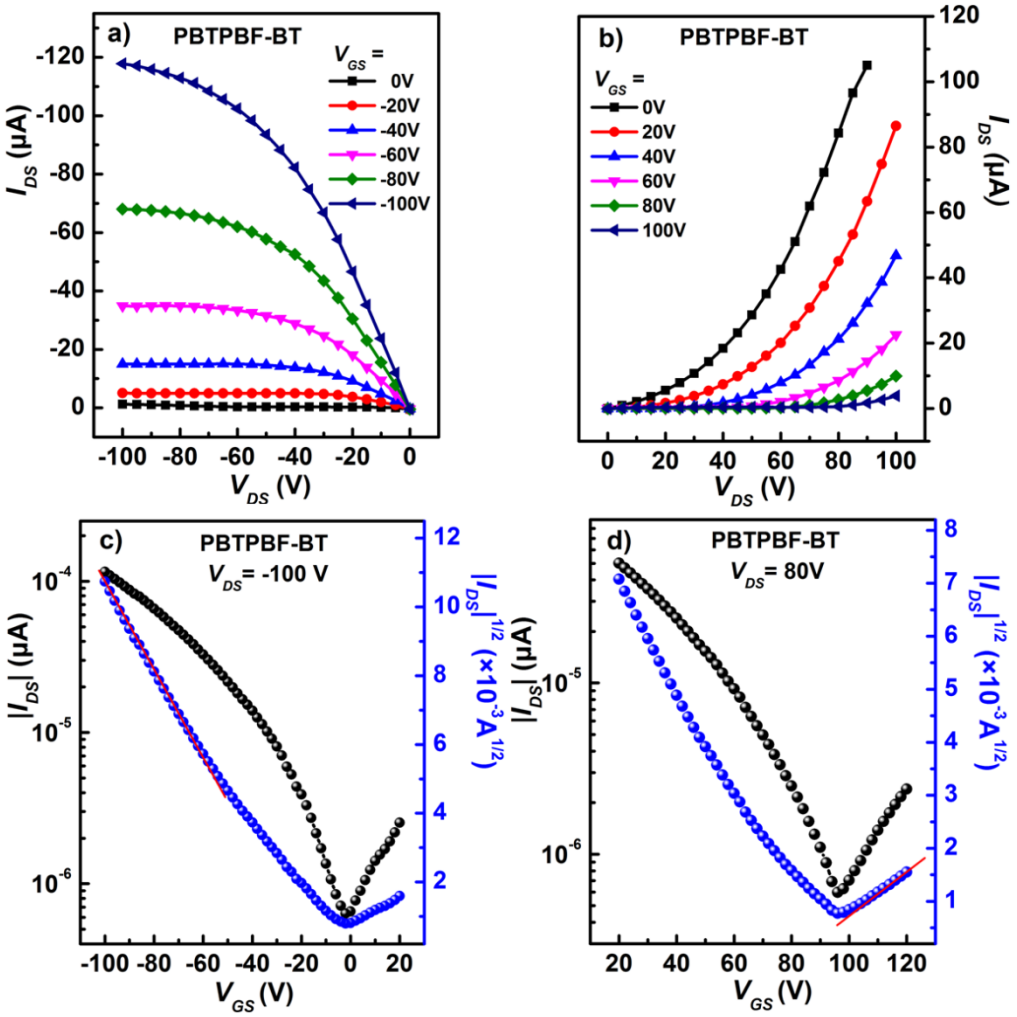

Fig. 7 Output (a, b) and (c, d) transfer characteristics of **PBTPBF-BT** annealed at 180 ^{o}C and tested under air conditions.

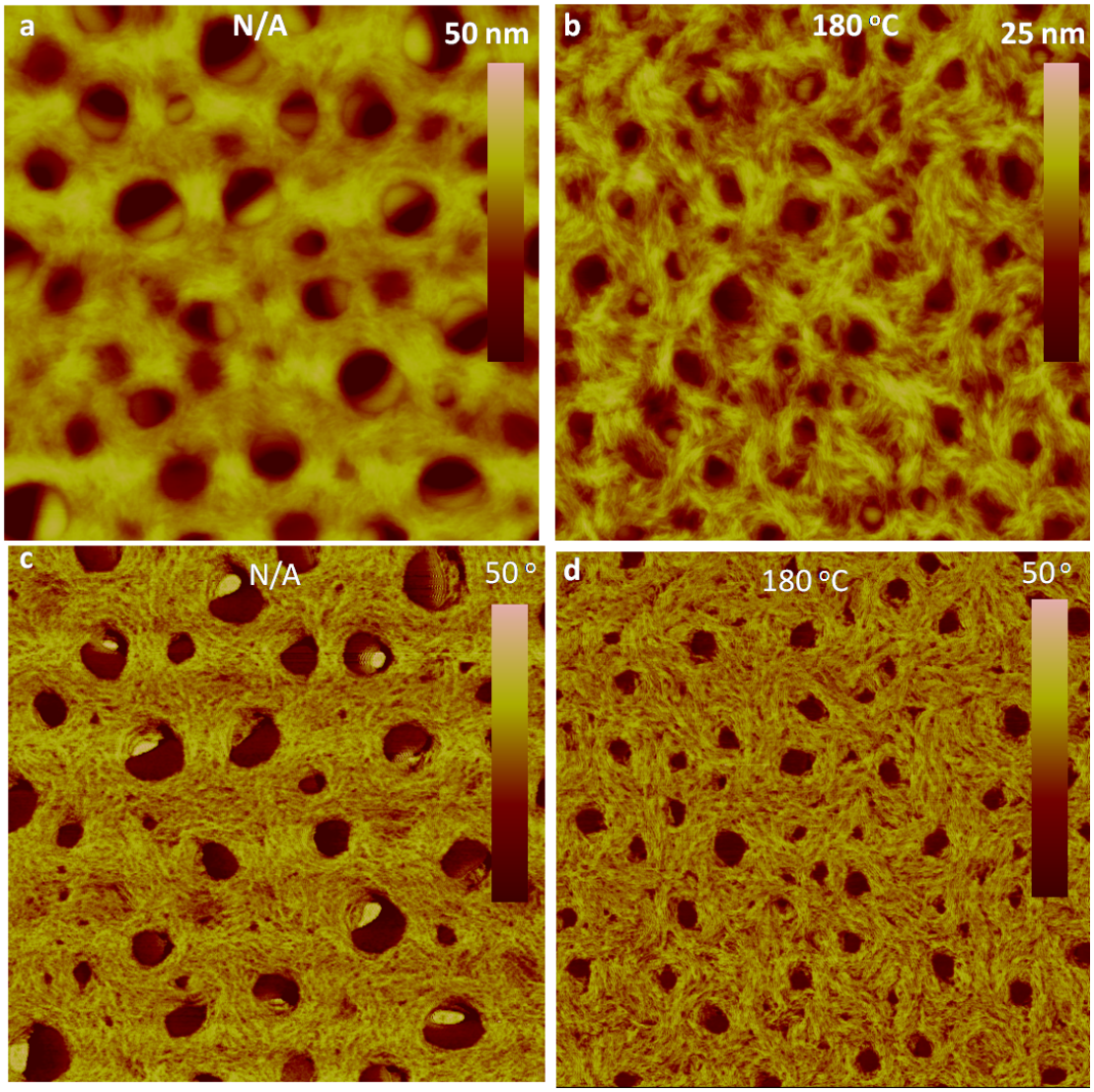

Fig. 8 AFM images (2 μm × 2 μm) of **PBTPBF-BT** thin film on Cytop-modified Si/SiO_2 substrates with and without annealing: height images (a and b), phase images (c and d).

Table 1. Optical and electrochemical properties of polymers

Polymer	λ_{max}^{abs} (nm)		λ_{onset}^{abs} (nm)	E_g^{opt}	E_{onset}^{red}	E_{onset}^{ox}	HOMO	LUMO
	Solution	Film	Film	(eV)[a]	(V)	(V)	(eV)[b]	(eV)[c]
PBTPBF-BT	1107	1107	1750	0.71	–0.81	0.43	–5.18	–3.94
PBIBDF-BT[d]	811	823	1047	1.18	–0.68	0.84	–5.55	–4.03

[a] E_g^{opt} =1240/ λ_{onset}^{abs} (in film), [b] HOMO = –(4.75+ E_{onset}^{ox}), [c] LUMO = –(4.75+ E_{onset}^{red}). [d] Values of the isoindigo derivative-based polymer were referred 12a.

Electronic Supplementary Information

A new thieno-isoindigo derivative-based D–A polymer with very low bandgap for high-performance ambipolar organic thin-film transistors

Guobing Zhang,[a, c]* Zhiwei Ye,[a] Peng Li,[a, b] Jinghua Guo, [a, b] Longxiang Tang,[b] Hongbo Lu,[a, c] and Longzhen Qiu [a, c]*

[a]Key Lab of Special Display Technology, Ministry of Education, National Engineering Lab of Special Display Technology, State Key Lab of Advanced Display Technology, Academy of Opto-Electronic Technology, Hefei University of Technology, Hefei, 230009, China. E-mail: gbzhang@hfut.edu.cn, lzqiu@ustc.edu

[b]Department of Polymer Science and Engineering, School of Chemistry and Chemical Engineering, Hefei University of Technology, Hefei, 230009, China.

[c]Anhui Key Laboratory of Advanced Functional Materials and Devices, Hefei University of Technology, Hefei, 230009, China.

1. **Characterization (Table S1-S3. Fig. S1-S5)**
2. **NMR spectra (Fig. S6-Fig. S11)**
3. **Mass spectrum and DSC of new monomers (Fig. S12-S14)**
4. **GPC results (Fig. S15)**

Table S1 Crystallographic parameters for polymer films of **PBTPBF-BT** and **PBIBDF-BT**.

Polymer	Lamellar spacing		π-π spacing	
	2θ (°)	d (Å)	2θ (°)	d (Å)
PBTPBF-BT	3.36	26.3	25.28	3.52
PBIBDF-BT[a]	-	28.5	-	3.55

[a] Values of the isoindigo derivative-based polymer were referred 12a.

Table S2 OTFTs performances of the polymers tested under vacuum.

Polymer	**T-annealing [°C]**	**Evaluation under vacuum conditions**					
		μ_h **(average)**[a] **[$cm^2V^{-1}s^{-1}$]**	I_{on}/I_{off}[b]	V_{th} **[V]**	μ_e **(average)**[a] **[$cm^2V^{-1}s^{-1}$]**	I_{on}/I_{off}[c]	V_{th} **[V]**
PBIBDF-BT	N/A	_	_	_	0.46 (0.29)	$10^4 – 10^5$	-0.4
	180	_	_	_	1.06 (0.79)	$10^4 – 10^5$	28.7
PBTPBF-BT	N/A	0.13 (0.10)	$10^2 – 10^3$	-15.5	0.08 (0.07)	$10^2 – 10^3$	47.0
	150	0.34 (0.30)	$10^3 – 10^4$	-26.4	0.13 (0.10)	$10^2 – 10^3$	55.6
	180	0.45 (0.38)	$10^4 – 10^5$	-21.3	0.22 (0.18)	$10^3 – 10^4$	56.9

[a]Average mobility from more than 8-10 devices; [b]Evaluated at V_D = –20 V; [c]Evaluated at V_D = +20 V.

Table S3 OTFTs performances of the polymers tested under air.

Polymer	T-annealing [°C]	Evaluation under air conditions					
		μ_h (average)[a] [$cm^2V^{-1}s^{-1}$]	I_{on}/I_{off}[b]	V_{th} [V]	μ_e (average)[a] [$cm^2V^{-1}s^{-1}$]	I_{on}/I_{off}[c]	V_{th} [V]
PBIBDF-BT[d]	N/A	0.39 (0.27)	$10^3 – 10^4$	-15.4	0.28 (0.20)	$10^3 – 10^4$	1.63
	180	0.36 (0.23)	$10^3 – 10^4$	-23	0.60 (0.37)	$10^3 – 10^4$	37.8
PBTPBF-BT	N/A	0.25 (0.21)	$10^3 – 10^4$	-19.5	0.03 (0.02)	$10^2 – 10^3$	76.6
	150	0.45 (0.36)	$10^2 – 10^3$	-14.4	0.02 (0.01)	$10^2 – 10^3$	69.1
	180	0.61 (0.53)	$10^2 – 10^3$	-16.2	0.07 (0.06)	$10^2 – 10^3$	76.2

[a] Average mobility from more than 8-10 devices; [b] Evaluated at V_D = –20 V; [c] Evaluated at V_D = +20 V. [d] The mobilities lower than those of the previous report (tested in low vacuum or glovebox, 12a).

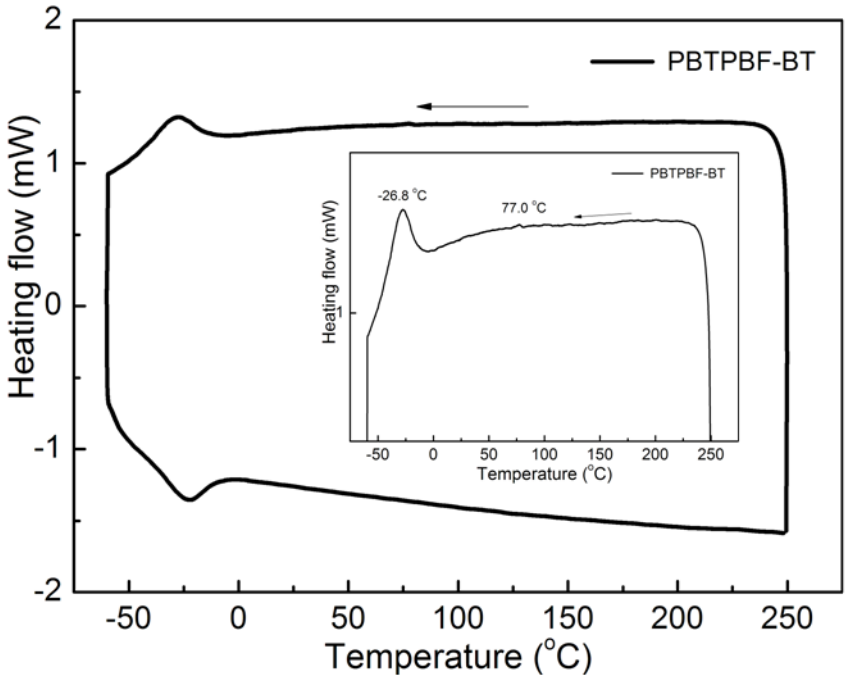

Fig. S1 The DSC curve of PBTPBF-BT.

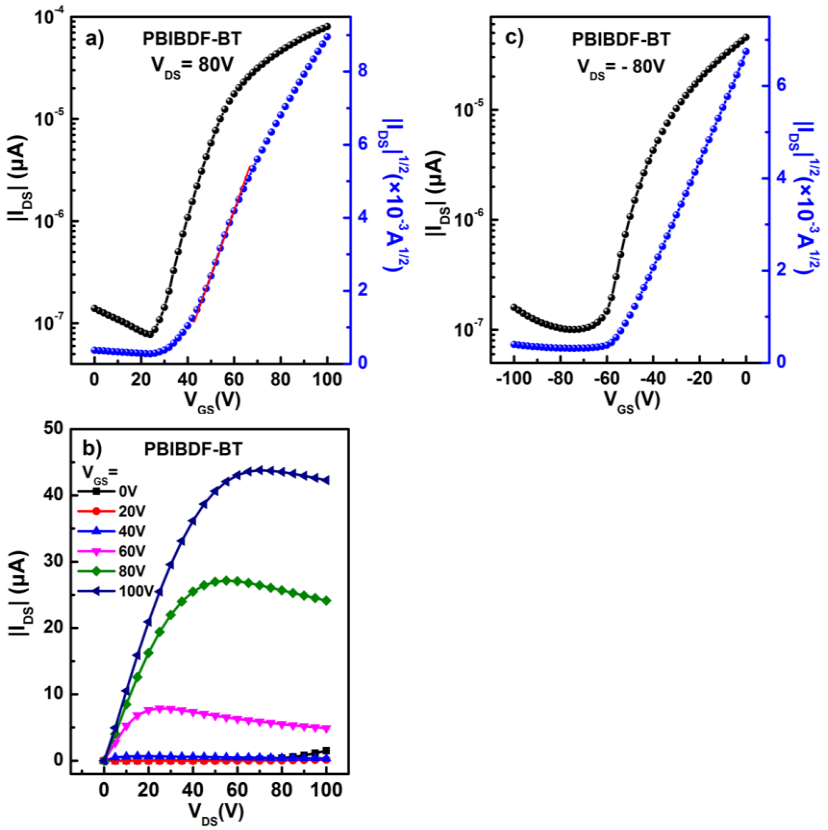

Fig. S2 the Output and transfer curves of **PBIBDF-BT** devices annealed at 180 °C and tested under vacuum. **PBIBDF-BT** exhibited n-channel transport in the vacuum with the electron mobility as high as 1.06 $cm^2V^{-1}s^{-1}$.

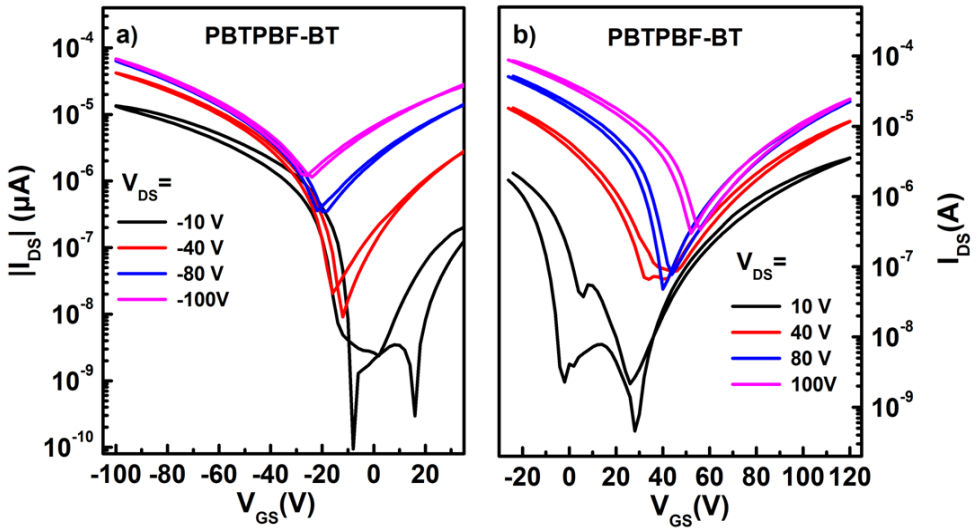

Fig. S3 The transfer characteristics of **PBIPBF-BT** devices annealed at 180 ^{o}C and test under vacuum condition. All the transfer curves for electron and hole transport showed negligible hysteresis.

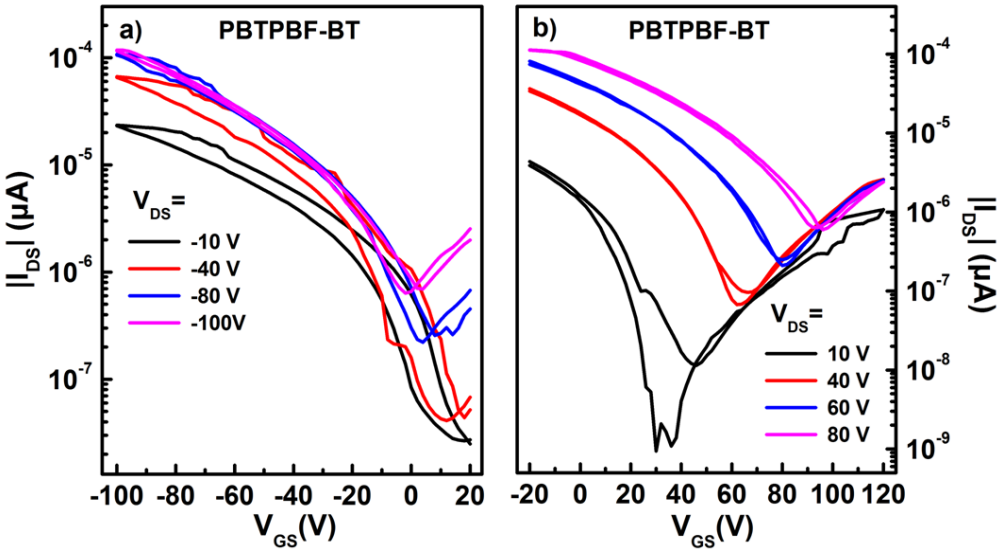

Fig. S4 The transfer characteristics of **PBIPBF-BT** devices annealed at 180 ^{o}C and test under air condition.

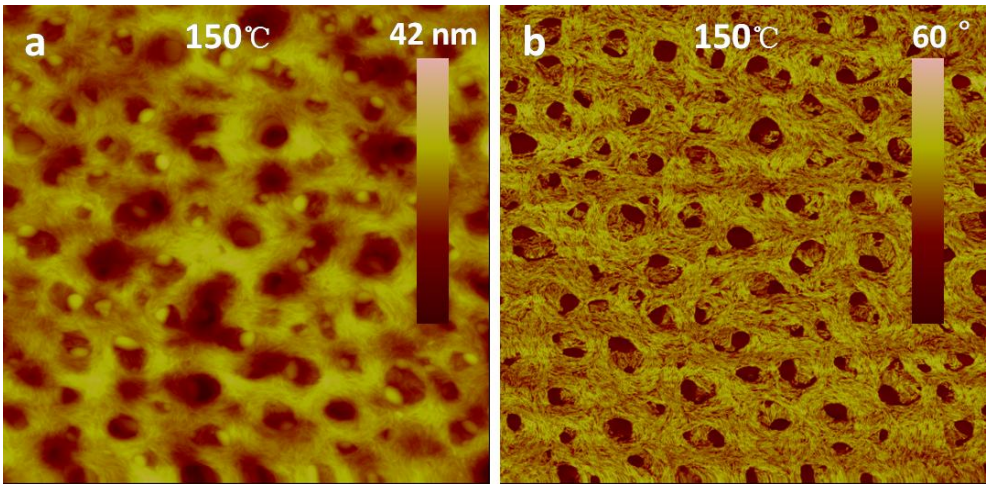

Fig. S5 AFM images (2 μm × 2 μm) of PBTPBF-BT thin film with the annealing temperature of 150 °C.

2. NMR spectra

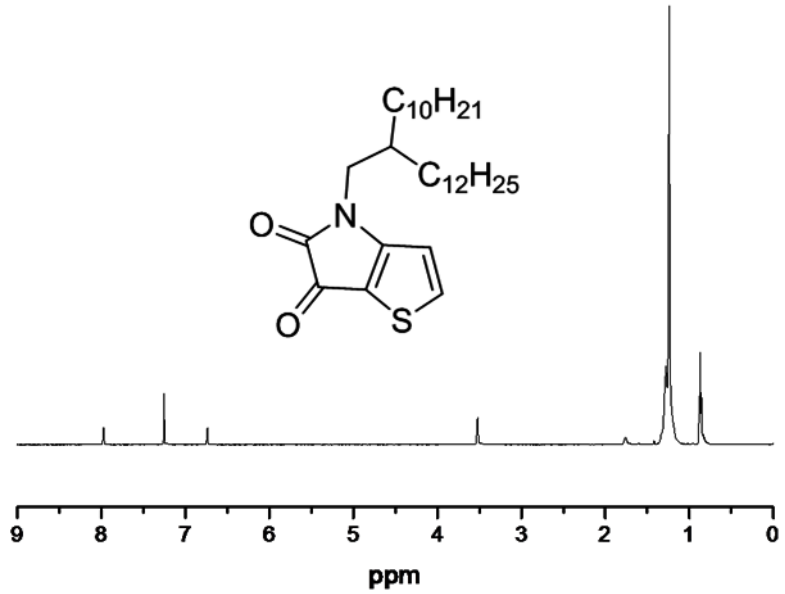

Fig. S6 ^{1}H NMR spectra of compound **2** in $CDCl_3$.

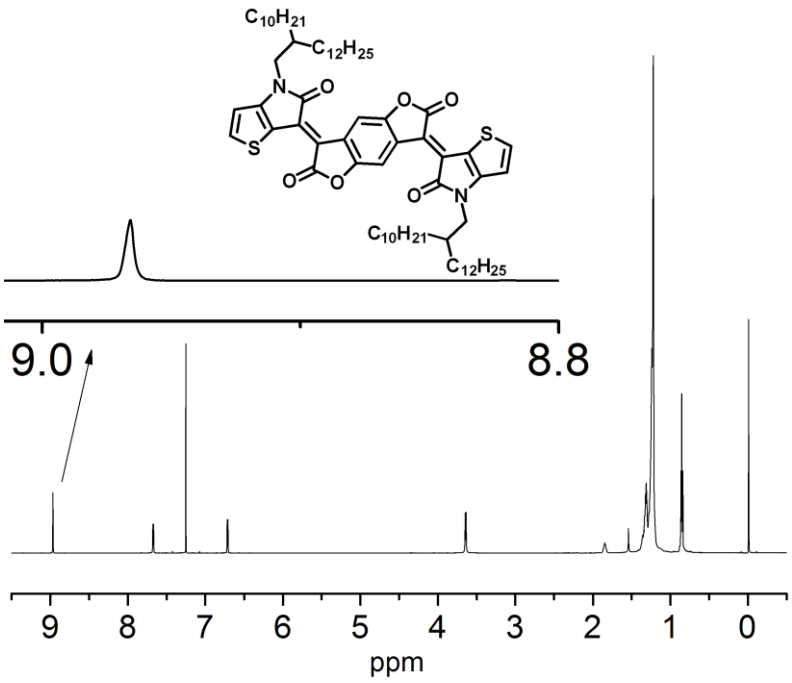

Fig. S7 ^{1}H NMR spectra of compound **3** in $CDCl_3$.

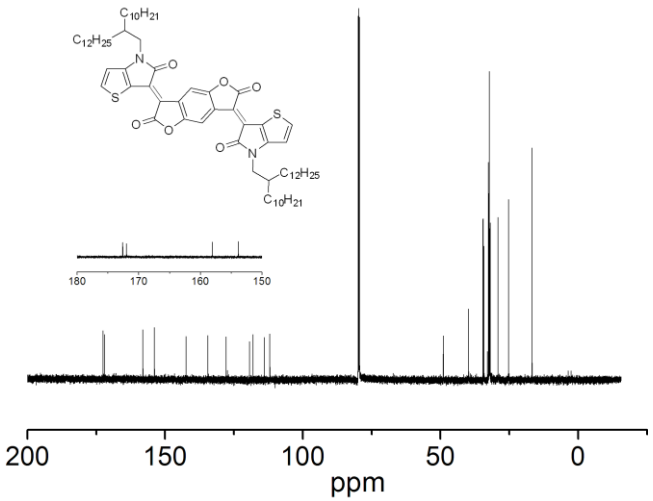

Fig. S8 ^{13}C NMR spectra of compound **3** in $CDCl_3$.

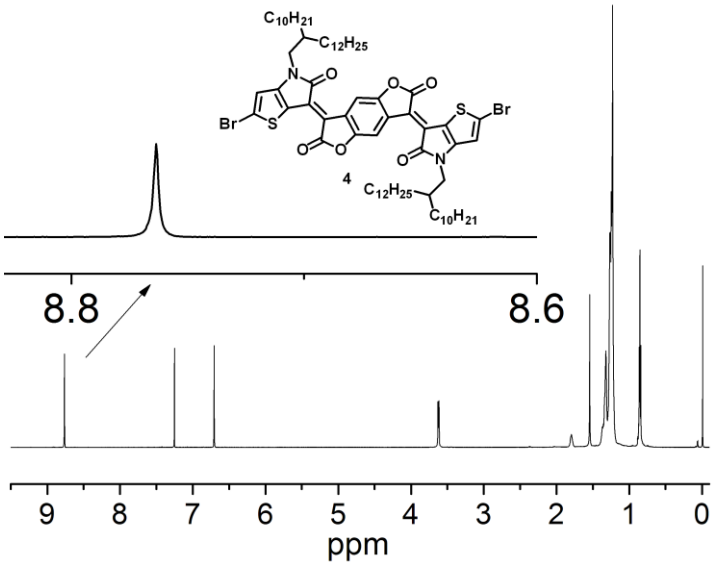

Fig. S9 ^{1}H NMR spectra of compound **4** in $CDCl_3$.

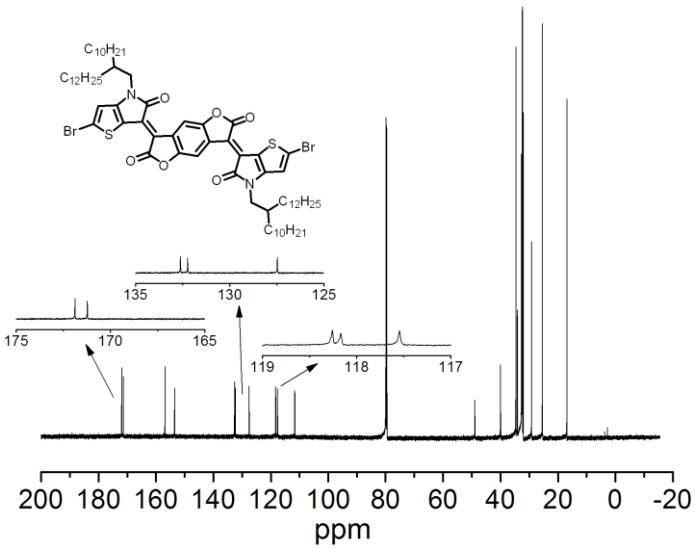

Fig. S10 ^{13}C NMR spectra of compound **4** in $CDCl_3$.

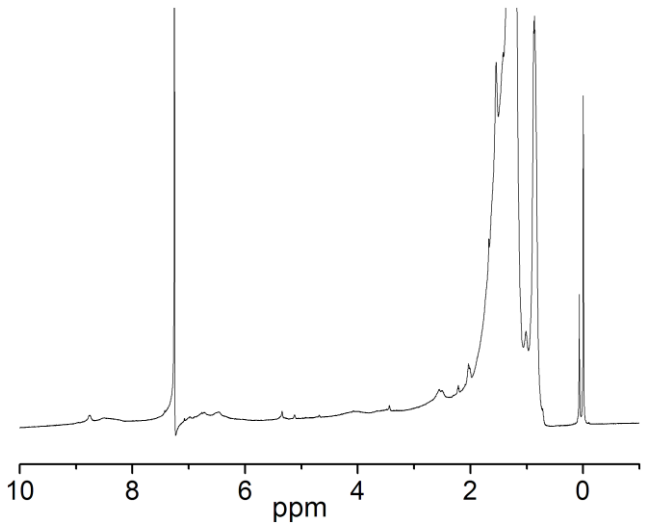

Fig. S11 ^{1}H NMR of **PBTPBF-BT**.

3. Mass spectrum and DSC curves of monomers

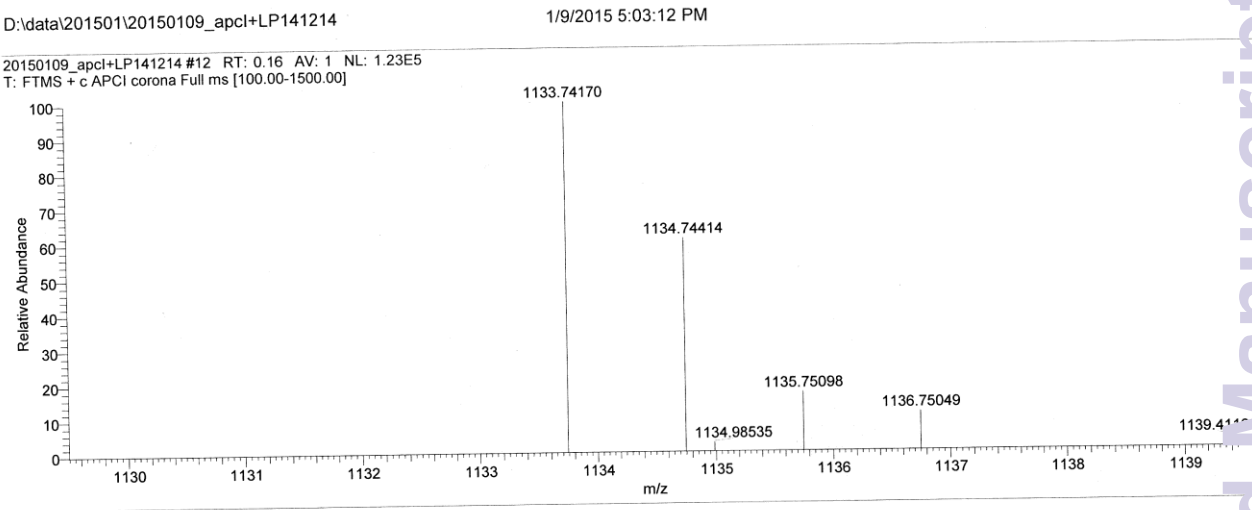

20150109_apcI+LP141214#12 RT: 0.16
T: FTMS + c APCI corona Full ms [100.00-1500.00]
m/z= 1129.49593-1139.46163

m/z	Intensity	Relative	Theo. Mass	Delta (mmu)	Composition
1133.74170	123272.9	100.00	1133.74086	0.84	$C_{70}H_{105}O_6N_2S_2$

Fig. S12 The mass spectrum of compound **3**.

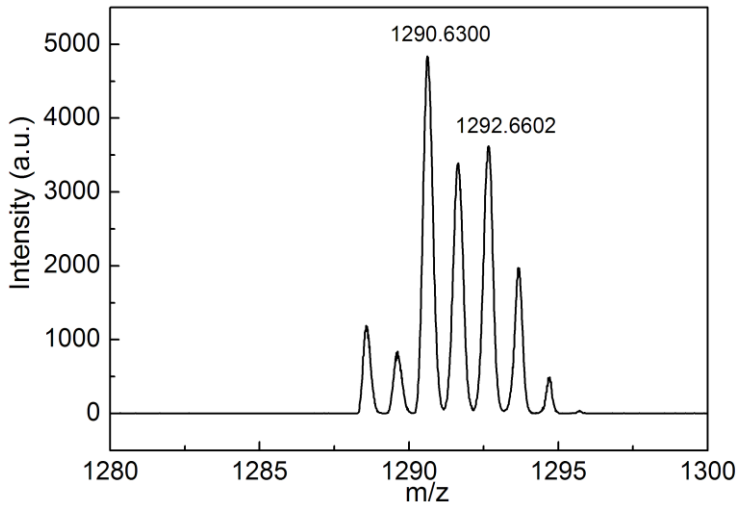

Fig. S13 The mass spectrum (MALDI-TOF) of **4**.

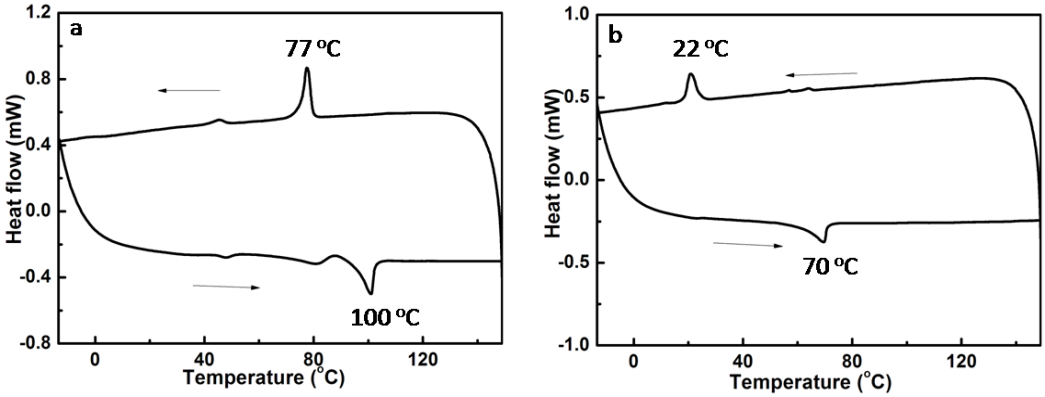

Fig. S14 The DSC curves of (a): compound **3** and (b): compound **4**.

4. GPC results

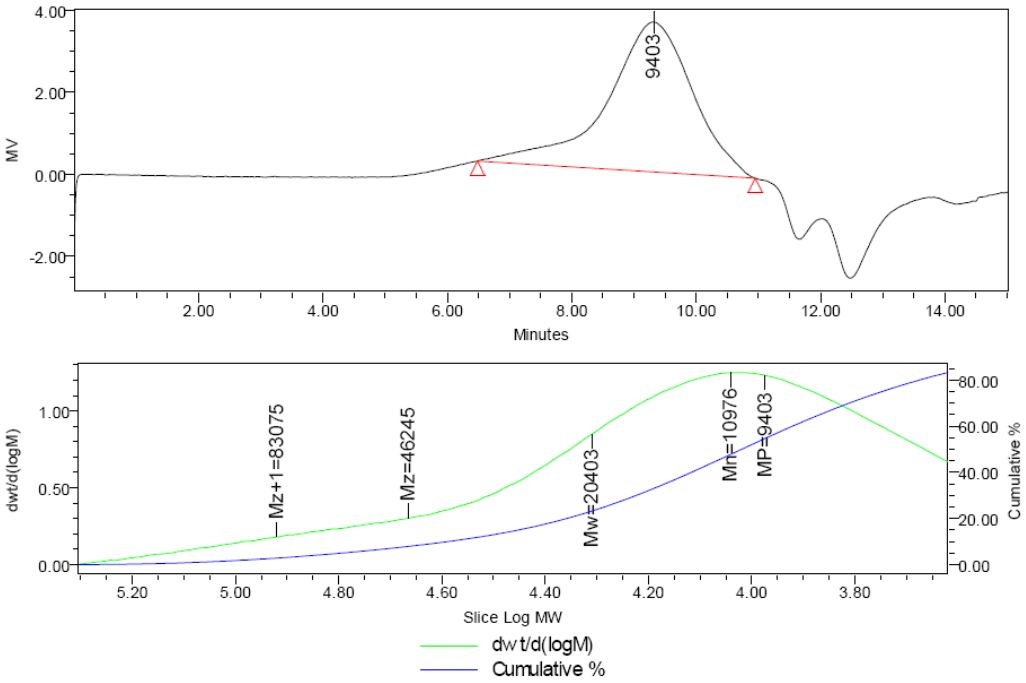

GPC Sample Results

	Retention Time	Mn	Mw	MP	Mz	Poly-dispersity
1	9.317	10976	20403	9403	46245	1.859

Fig. S15 GPC results of **PBTPBF-BT**.